Respiratory Research

RESEARCH

Open Access

Single-cell transcriptomics reveals e-cigarette vapor-induced airway epithelial remodeling and injury

Weitao Cao[1,2,3,4†], Jia Li[1,2,8†], Li Che[1,2,3,4†], Ruixue Yang[1,2,3,4†], Zehong Wu[5†], Guoping Hu[6], Weifeng Zou[7], Zehang Zhao[1], Yumin Zhou[1], Xingtao Jiang[5], Tiejun Zhang[1,9*], Wenguang Yin[1,2,3,4*] and Pixin Ran[1,2*]

Abstract

Background In recent years, e-cigarettes have been used as alternatives among adult smokers. However, the impact of e-cigarette use on human bronchial epithelial (HBE) cells remains controversial.

Methods We collected primary HBE cells of healthy nonsmokers and chronic obstructive pulmonary disease (COPD) smokers, and analyzed the impact of e- cigarette vapor extract (ECE) or cigarette smoke extract (CSE) on HBE cell differentiation and injury by single-cell RNA sequencing, immunostaining, HE staining, qPCR and ELISA. We obtained serum and sputum from healthy non- smokers, smokers and e-cigarette users, and analyzed cell injury markers and mucin proteins.

Results ECE treatment led to a distinct differentiation program of ciliated cells and unique patterns of their cell–cell communications compared with CSE. ECE treatment caused increased Notch signaling strength in a ciliated cell subpopulation, and HBE cell remodeling and injury including hypoplasia of ciliated cells and club cells, and shorter cilia. ECE-induced hypoplasia of ciliated cells and shorter cilia were ameliorated by the Notch signaling inhibition.

Conclusions This study reveals distinct characteristics in e-cigarette vapor-induced airway epithelial remodeling, pointing to Notch signaling pathway as a potential targeted intervention for e-cigarette vapor-caused ciliated cell differentiation defects and cilia injury. In addition, a decrease in SCGB1A1 proteins is associated with e- cigarette users, indicating a potential lung injury marker for e-cigarette users.

Keywords E-cigarette, COPD, Ciliated cells, Cilia, Notch signaling

Introduction

The airway epithelium, composed of basal cells, multiciliated cells, club cells, goblet cells and several rare cell types, is the primary site for pulmonary diseases including chronic obstructive pulmonary disease (COPD), the third cause of death in the world by 2030 according to the prediction by WHO (https://www.emro.who.int/health-topics/chronic-obstructive-pulmonary-disease-copd/index.html). Tobacco smoking can cause airway epithelial remodeling including multiciliated cell hypoplasia, goblet cell hyperplasia and mucus overproduction and is the leading cause of COPD.

†Weitao Cao, Jia Li, Li Che, Ruixue Yang and Zehong Wu contributed equally to this work.

*Correspondence:
Tiejun Zhang
zhang_tiejun@gzhmu.edu.cn
Wenguang Yin
yin_wenguang@gzhmu.edu.cn
Pixin Ran
pxran@gzhmu.edu.cn
Full list of author information is available at the end of the article

In recent years, e-cigarettes have been used as alternatives among adult smokers. However, unregulated marketing of e-cigarettes leads to increased prevalence of smoking in children and lower initial age of smoking onset. Studies on pulmonary effects of e-cigarette use have been focused on inflammatory response, epithelial barrier integrity and physiological changes. It has been shown that e-cigarette users exhibit an altered profile of innate immune proteins, protease–antiprotease imbalance and/or increased production of MUC5AC but not MUC5B [1–3]. E-cigarette vapor impairs airway mucociliary function, lung function and pulmonary tissue destruction, and also alters lung lipid homeostasis in experimental animals [4–6]. Additionally, e-cigarette use also increases blood pressure, aortic stiffness and heart rate [7].

Several bulk transcriptomic studies reveal that e-cigarette use or vapor exposure alters gene expression profiles in respiratory cells or tissues. For example, exposure of differentiated human bronchial epithelial (HBE) cell cultures to e-cigarette vapor leads to altered gene expression patterns of phospholipid and fatty acid triacylglycerol metabolism pathways, inflammatory genes, ribosomal protein genes and cilia-related genes [8–10]. Exposure of HBE cells to flavoring chemicals such as diacetyl and 2,3- pentanedione found in e-cigarette can also decrease expression of genes related to ciliogenesis and leads to reduced number of ciliated cells [11]. These data suggest that e-cigarette exposure may affect cilia function and/or the cilia structure formation. In addition, nasal scrape biopsies from e-cigarette users shows decreased RNA expression of immune-related genes [12]. However, how e-cigarette affects human airway epithelial cells in detail, especially ciliated cell subtype differentiation and the cilia structure including cilia length remains unclear.

Here, we investigate the potential effects of e-cigarette vapor extract (ECE) on HBE cells from healthy nonsmokers and COPD smokers. For reference, we also examined the effects of cigarette smoke extract (CSE). We exposed HBE cells cultured in vitro at an air–liquid interface (ALI) to ECE or CSE with an equal nicotine concentration. To overcome the limitations of bulk tissue analyses, we used single- cell RNA sequencing (scRNA-Seq) technology to profile the transcriptomes of individual HBE cells in ALI cultures. We also characterized the effects of ECE or CSE on HBE cells by using immunostaining, HE staining, qPCR and ELISA. These results reveal ECE-caused distinct remodeling and injury of bronchial ciliated cells for healthy nonsmokers and COPD patients, and indicate a potential therapeutic intervention of airway epithelial remodeling and injury caused by e-cigarette vapor by inhibiting Notch signaling.

Methods

Human bronchial brushing collection

Primary human bronchial epithelial (HBE) cells (material obtained from the Biobank of the First Affiliated Hospital of Guangzhou Medical University, Guangzhou, China, and approved the ethics committee of the First Affiliated Hospital of Guangzhou Medical University 2020-51) were obtained from brushings of 5–6-order bronchioles taken during fiberoptic bronchoscopy with an endoscopic cytobrush. COPD was confirmed by post-bronchodilator FEV1/FVC < 70%. Stages of COPD were classified by spirometric classification (GOLD III: 30% ≤ FEV1 < 50% predicted, GOLD IV: FEV1 < 30% predicted). Patients with asthma, bronchiectasis, pulmonary fibrosis or infection were excluded in this study. These information of healthy nonsmokers and COPD smokers is listed in the Supplementary Table 1 (Table S1).

Ethical approval

This study is conducted in accordance with the ethical guidelines outlined in the Declaration of Helsinki. This study has been approved by the institutional review board at the First Affiliated Hospital of Guangzhou Medical University. Informed written consents were obtained from all participants who agreed to participate in this study.

E-cigarettes and cigarettes

The e-cigarette system including a RELX Wuxian device and a pod with menthol flavor e-liquid was commercially available at the time of the study, and obtained from a retail store in Shenzhen, China. The main formulation of menthol-containing e- liquid mainly includes propylene glycol (PG) (35%), glycerol (51%), nicitone (4%), and flavors (10%). The wattage of the RELX Wuxian device was 6.5 Watt. A commercial combustible cigarette (Hongmei, Hongta Group, China) was obtained from a retail store in Guangzhou, China. Both of them were stored in an airtight container at room temperature until use.

CSE and ECE preparation

Aqueous extracts of the menthol-containing e-cigarette vapor and cigarette smoke (CS) were prepared with the following methods. A Cerulean CETI 8 MK3 smoking machine (CERULEAN, UK) was used to generate e-cigarette vapor and mainstream CS. The e-cigarette vapor and CS were generated according to the Cooperation.

Centre for Scientific Research Relative to Tobacco (CORESTA) Recommended Method No. 81 vaping regime (specifing a square-wave puff profile, 55 mL puff volume, 3 s duration and a 30 s interval) and ISO 20778:2018 method (specifing a 55 mL puff volume, 2 s

duration and a 30 s interval), respectively. The mainstream vapor or smoke was passed through the two collection vessels with 2*20 mLDMEM/F-12 medium, and then mixed and shaken for 20 min to obtain the aqueous extracts of e- cigarette vapor and CS for use. The nicotine concentration was determined by UPLC (Waters, US).

Measurement of component in CSE and ECE

The main components in the e-cigarette and cigarette smoke collected in the culture- medium extracts were also analyzed by gas chromatography–mass spectroscopy (GC- MS), and the results showed that there were significant differences in the main components from the two extracts (Table S2). The common component was nicotine with the content of 1304.9 (ECE) and 1022.7 (CSE) mg/kg, respectively (Table S2). The other major components of e-cigarette vapor collected in the culture-medium included PG, Gly, menthol racemic and ethyl alcohol which were basically the same as the main ingredients in e-cigarette liquid, excepting for benzoic acid below the limited of detection (Table S2). Other major components below the detection limit included acetic acid, acetone alcohol, dihydroxyacetone, etc., which can only be qualitatively identified by GC–MS due to their low content. The other main characteristic components in the cigarette smoke collected in the culture medium was glycerol triacetate, and other relatively rich ingredients including acetone, methyl acetate, 2-butanone, acetic acid, 1,3-dihydroxyacetone, phenol, acetic acid glyceride, et al. The pH values of CSE or ECE with an equal nicotine concentration of 0.02 mg/ml used for HBE cell exposure in this study is 7.66 and 7.74, respectively.

HBE cell ALI culture, and CES, ECE or chemical treatment

HBE cells were cultivated under air–liquid interface conditions to form well- differentiated, pseudostratified cultures as described previously [25]. Briefly, isolated HBE cells were maintained and expanded (one passage) inT75 flasks inbronchial epithelial cell expansion medium (05040, STEMCELL Technologies) at 37 °C in a 5% CO2 incubator. At 80% confluence, cells were detached with 0.05% trypsin–EDTA (Gibco) and seeded on membrane supports (12 mm Transwell culture inserts, 0.4 μm pore size, Costar) coated with 0.05 mg collagen from calf skin (Sigma-Aldrich) in ready-to-use AEGM supplemented with 1% penicillin/streptomycin. HBE cells were cultured for two days until they reached complete confluence. The apical medium was then removed and the basal medium was replaced by ALI culture medium (05001, STEMCELL Technologies). Cultures were maintained under air–liquid interface conditions by changing the medium in the basal filter chamber three times a week.

For CSE treatment, a1.023 $mg.mL^{-1}$stock solution was diluted to 0.02 $mg.mL^{-1}$. For ECE treatment, a 1.305 $mg.mL^{-1}$ stock solution was diluted to 0.02 $mg.mL^{-1}$. For DAPT (GSI-IX) treatment, a 25 $mg.mL^{-1}$stock solution was diluted to 10 μM. Epithelial cells were cultured in differentiation medium containing CSE or ECE at 37 °C in a 5% CO2 incubator from day 5 to day 14. For rescue experiment, epithelial cells were cultured in differentiation medium containing CSE or ECE at 37 °C in a 5% CO2 incubator from day 5 to day 14 and DAPT was added into medium from day 14 to day 21. The medium was replaced every 24 h before collection for analysis.

Single-cell RNA sequencing

HBE cell ALI cultures from 3 healthy nonsmokers or 3 COPD smokers were collected for single-cell analysis. Basic information of healthy nonsmokers and COPD patients were listed in the Supplementary Table 1 (Table S1). To obtain single-cell suspensions, cells were incubated in a mixture of collagenase D (1 $mg.mL^{-1}$), elastase (1 $mg.mL^{-1}$), dispase (50 $U.mL^{-1}$) and DNase I (0.1 $mg.mL^{-1}$) in HBSS for 1 h at 37 °C while shaking. Enzyme activity was inhibited by adding HBSS containing 10% fetal bovine serum (FBS). Dissociated cells in suspension was forced to pass through a 40-μm cell strainer (Falcon) and then centrifuged at 500 g for 5 min at 4 °C. The cell pellet was resuspended to incubate in red blood cell lysis buffer for 2 min at room temperature. After adding HBSS containing 10% FBS into the suspension, the mix was centrifuged at 300 *g* for 5 min at 4 °C. Finally, the cell pellet resuspended in 500 μl of ice-cold HBSS. Cell concentration was measured by using a Countess automated cell counter (Thermo Fisher Scientific). Cell viability was examined by using a Countess automated cell counter (Thermo Fisher Scientific). Cells were captured by using the 10×genomics device. Cellranger 6.0 was used to demultiplex raw data to fastq files and count raw counts (using GRCh38 as reference) for each gene in each cell. Seurat 4.0 was used to preprocessing the data, perform quality control and filter out low quality cells. We filtered out the cells with detected genes number less than 200 and mitochondria percentage larger than 10%. We also removed the genes that detected in less than 50 cells. Doublet was detected and removed by using DoubletFinder. Scanpy (https://scanpy.readthedocs.io/en/stable/) was used to integrate and visualize cell clusters. Specifically, we normalize library size by dividing raw counts by total molecules per cell. Pseudocount was log- transformed. Highly variable genes were identified using pp.highly_variable_genes function, which was further used for downstream clustering. Principal components (PCs) were calculated using the

selected highly variable genes. To remove batch effect, BBKNN was used to integrate data from mice with different treatment. After computing the neighborhood graph (pp.neighbors), dimension reduction via UMAP was performed by running tl.umap functions. Cluster marker genes were obtained by ranking the highly differential genes in each cluster (tl.rank_genes_groups). scVelo [39] was used to perform RNA velocity analysis and infer cell differentiation paths and latent-time. Cell–cell communication analysis was performed using CellChat [19].

Immunostaining of HBE cells

ALI cultures were fixed in 4% paraformaldehyde 20 min at RT, followed by incubation in permeabilization solution (0.3% Triton X-100/PBS) for 15 min and in blocking solution (5% FBS/PBS/3% BSA) for 1 h at RT, incubated in primary antibodies overnight at 4 °C, washed, incubated in secondary antibodies for 2 h at RT, washed, and then mounted for imaging.

Reverse transcription quantitative PCR (RT-qPCR)

Total RNA extraction was conducted using a miRNeasy Mini Kit (Qiagen, 217004). cDNA was synthesized using the Maxima First Strand cDNA Synthesis Kit (Thermo Fisher Scientific, K1641), according to manufacturer's instructions. Quantitative real- time PCR was performed using ChamQ Universal SYBR qPCR Master Mix (Vazyme, Q711-02). The following primers were used: *hACTB* forward 5′- TCATTCCAAATATGAGATGCG TTG -3′ and *hACTB* reverse 5′- TAGAGAGAAGTG GGGTGGCT -3′;*hFOXJ1* forward 5′-TCTGAGCCA GGCACCACATA -3′ and *hFOXJ1* reverse 5′- CCATGT CTGCGGGGACTCT-3′.

ELISA

SCGB1A1 or MUC5AC levels in supernatant of HBE cells at the ALI, human serum or sputum were measured by a sandwich enzyme-linked immunosorbent assay (ELISA) using the SCGB1A1 ELISA Kit (Biovendor, RD191022200) or the MUC5AC ELISA Kit (Elabscience, E-EL-H2279) accounting to manufacturer's instructions, respectively.

Antibodies

The following antibodies were used: Mouse Anti-Acetylated α-Tubulin (1:1000, Sigma, T7451); Rabbit anti-MUC5AC (1:200 for IF, 1:10000 for WB, Abcam, ab3649); Rabbit anti-SCGB1A1 (1:400, Biovendor, RD181022220); Rabbit anti-Ki67 (1:400, Thermo, PA5-19462); Mouse anti-CDH1 (1:400, bdbiosciences,610181); Mouse anti-P63 (1:400, Abcam, ab735); Rabbit anti-MUC5B (1:5000, Novus Biologicals, NBP1-92151).

Imaging

Imaging of ALI cultures was performed using a Zeiss 880 upright laser scanning confocal microscope (Carl Zeiss Microscopy GmbH). Quantification of cell number was performed using ImageJ (http://rsbweb.nih.gov/ij/).

Quantification of immunofluorescence stained HBE cells

For each sample, 3 random fields were selected for cell counting of $DAPI^+$ total cells, $MUC5AC^+$ goblet cells, $TP63^+$ basal cells, $CDH1^+$ epithelial cells, acetylated α- $Tubulin^+$ ciliated cells and $SCGB1A1^+$ club cells. For each patient, control groups were normalized 1.

Cilia length measurements

To measure cilia length in HE staining, 4–5 random fields were captured from HE- stained cross sections from each donor in duplicate. The straight-line lengths of individual cilia in 5–6 ciliated cells per field (1 cilium per cell) were measured using SPOT Pro Plus Imaging Solutions software (Diagnostic Instruments Inc., Sterling Heights, MI) [40].

Statistical analysis

Experiments were performed in triplicate and repeated three times. Statistical analyses were performed using GraphPad software. For comparisons between two groups, a two-tailed Student's t-test was used. Comparisons among three groups were performed by one-way ANOVA, followed by a Tukey's multiple comparison test. A p-value of < 0 0.05 was considered to be statistically significant. Data are expressed as mean ± standard error of the mean.

Results

Identification of bronchial epithelial cell subpopulations in ALI cultures of healthy nonsmoker and COPD smokers treated by e-cigarette vapor extract (ECE) or cigarette smoke extract (CSE)

Epithelial cells from 5–6-order bronchioles of healthy nonsmokers and COPD smokers were collected by brushing. After expansion, epithelial cells were seeded onto transwell filters and the medium from the upper chamber was removed to initiate cell differentiation at air–liquid interface (ALI) for 5 days. ALI cultures were then exposed to e-cigarette vapor extract (ECE) or cigarette smoke extract (CSE) with an equal nicotine concentration of 0.02 mg/ml determined by ultra-performance liquid chromatography followed by samples collection for experiments and data analysis.

For single cell RNA sequencing of HBE cells, doublet and low-quality cells were removed, leaving total

41,215 single cells from six groups (healthy nonsmoker ALI cultures (healthy): 7563 cells; healthy nonsmoker ALI cultures exposed to ECE (healthy + ECE): 5121 cells; healthy nonsmoker ALI cultures exposed to CSE (healthy + CSE): 6588 cells; COPD smoker ALI cultures (COPD): 7,185 cells; COPD smoker ALI cultures exposed to ECE (COPD + ECE): 7560 cells; COPD smoker ALI cultures exposed to CSE (COPD + CSE): 7198 cells. Using

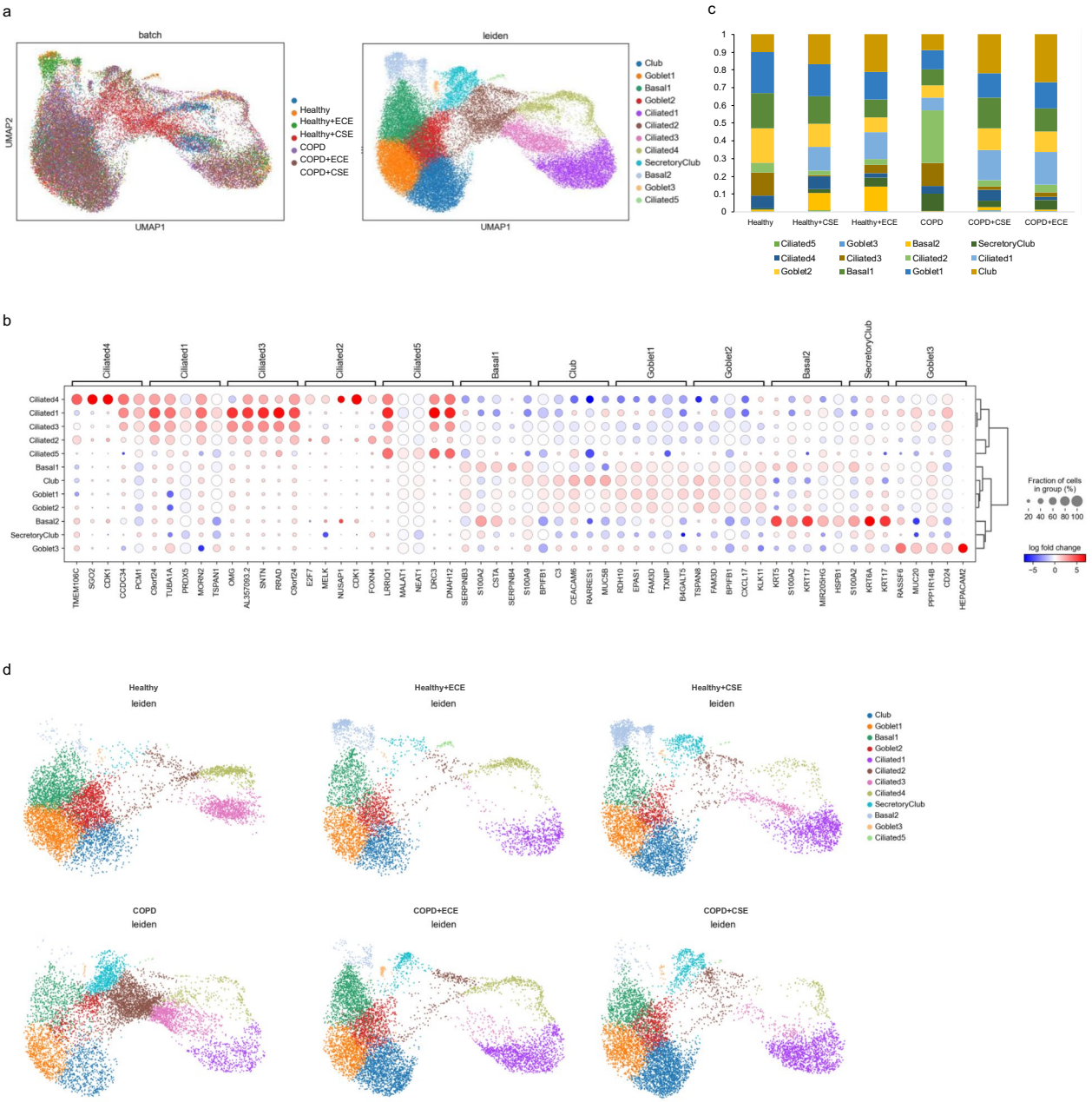

Fig. 1 Single-cell RNA-seq data analysis reveals changes in HBE cell populations upon ECE or CSE treatment. **a** UMAP embedding representation of single-cell transcriptomes of ALI cultured HBE cells from healthy nonsmokers and COPD smokers treated with ECE and CSE, respectively, colored by treatments (the left panel) and cell types (the right panel). **b** Bubble plot showing the top5 marker genes for each cell type. Colors and size represented the log2fold change and percentage of cells expressing the gene, respectively. **c** Ratio of each ALI cultured HBE cell type from healthy nonsmokers and COPD smokers treated with ECE and CSE, respectively. **d** UMAP projections of cells from ECE-treated or CSE-treated ALI cultures from healthy nonsmoker or COPD smokers. Colors represented cell types. UMAP: Uniform Manifold Approximation and Projection; COPD: chronic obstructive pulmonary disease; CSE: cigarette smoke extract; ECE: e-cigarette vapor extract. HBE: human bronchial epithelial

unsupervised clustering and canonical markers [13], we identified basal cell populations highly expressing *KRT17* and *KRT5* (basal1 and basal2 clusters), club cell populations highly expressing *MUC5B* and *SCGB1A1* (club cell and secretory club cell clusters), goblet cell populations highly expressing *MUC5AC* and *TSPAN8* genes (goblet1,2,3 clusters) and ciliated cell populations highly expressing *FOXJ1* and *TUBB4B* (ciliated 1, 2, 3, 4, 5 clusters) (Fig. 1a and b and supplementary figure S1a and b). Interestingly, we observed that most of cells in the populations of club cells, goblet cells and basal cells were in the S phase, indicating that they are replicating their DNA (Fig S1c).

To further characterize the effect of ECE or CSE treatment on changes of cell populations, we calculated cell fractions for each group. The percentage of club cells in ALI cultures was increased from 10 to 17% or 21% after ECE or CSE treatment in healthy nonsmoker ALI cultures, respectively (Fig. 1c and d). Similarly, the percentage of club cells in ALI cultures was increased from 9 to 22% or 27% after ECE or CSE treatment in COPD smoker ALI cultures, respectively (Fig. 1c and d). We identified five ciliated cell subclusters. The ciliated4 cluster expressed *PLK4*, *DEUP1*, *FOXN4* and *CENPJ* indicating its early ciliating state (centriole assembly) [13] (supplementary figure S2a). Most of ciliated4 cells were at the G2/M phase, suggesting that they are actively proliferating or at early ciliating stages (supplementary figure S1c). ECE treatment appeared to not significantly alter ciliated4 cell fractions in healthy nonsmoker or COPD smoker ALI cultures (Fig. 1c and d). However, the percentage of ciliated4 cells was dramatically decreased in CSE treatment groups, from 7.2% to 2.4% for healthy nonsmokers and from 4.3% to 1.9% for COPD smokers compared with controls, respectively (Fig. 1c and d). Ciliated1 and ciliated5 clusters expressed *RSPH1*, *SPAG1*, *DNALI1* and *IFT57*, indicating that they are at the mature stage (axonemalfunction and maintenance) (supplementary Fig. 2b) [14]. The ciliated3 cluster had a premature transcriptome profile compared with ciliated1 cluster, characterized by a lower expression of *FOXJ1* and *TUBB4B*(supplementary figure S1b). The ciliated2 cluster expressed both secretory markers, such as *SCGB3A1* and basal cell signature genes, such as *CEACAM6*, *TGM2* and *CP* (Supplementary Fig. 2c and d).

Relationships within bronchial ciliated cell subpopulations in ALI cultures of healthy nonsmoker and COPD smoker treated by ECE or CSE

Next, we characterized differences of pseudotime trajectory ciliated cells among these six groups. We subseted these five ciliated cell clusters and performed pseudotime trajectory analysis (Fig. 2a–d). Latent time analysis showed that both ECE and CSE treatment led to impaired differentiation of ciliated cells (Fig. 2b). In general, the partition-based graph abstraction (PAGA) velocity-graph analysis showed that ciliated2 could be pre-ciliated or ciliated progenitor cells, which had two differentiation paths: one towards ciliated3 and the other towards ciliated4, which could further differentiate into ciliated1 (Fig. 2c). Ciliated1 cells expressed mature ciliated markers, such as *RSPH1*, *CDHR3* and *DNALI1* (Fig. 2c and supplementary figure S2b) [14, 15]. Ciliated2 and 3 cells expressed basal and club cell signature genes, such as *BPIFB1* and *SERPINB3* (supplementary figure S2e). The majority of ciliated2 and 3 cells were from COPD smoker non-treatment ALI cultures, suggesting that COPD smoker ALI cultures may have enriched pre-ciliated cells as basal cells can differentiate into club cells which could continue to differentiate into ciliated cells (Fig. 2a) [16].

Next, we identified key genes related to ciliated cell differentiation that were affected by ECE or CSE treatment (Fig. 2d). CSE treatment caused an accumulation of a pre-ciliated status in both healthy nonsmoker and COPD smoker groups (Fig. 2d). ECE treatment led to a less pre-ciliated status, which was in the middle of pseudotime stage between the pre-ciliated (CSE treatment) and mature status (non-treatment) (Fig. 2d). For example, pre-ciliated marker genes*FANK1* were highly expressed in the CSE treatment group, with medium levels in the ECE treatment group and lowest expression in the non-treatment group in healthy nonsmoker ALI

(See figure on next page.)

Fig. 2 Pseudo-time analysis uncovers abnormal ciliated cell differentiation paths upon ECE or CSE treatment. **a** UMAP plot representing ciliated cell populations, color-coded by ciliated cell subsets (left panel) and treatment groups (right panel). **b** Violin plot shows inferred latent time indicating differentiation status for ciliated cells from each treatment group. **c** PAGA velocity graph showing the major ciliated cells differentiation paths. **d** Heatmaps showing the dynamics of gene expression levels along pseudo-time trajectory for ciliated cells in each treatment group, color-coded by expression level. From left to right: under-differentiated to differentiated ciliated cell stages. Color bars represent the ciliate cell cluster in (a). **e** RNA velocity vectors projected onto the UMAP embedding, reflecting ciliated cells differentiation paths. **f** Key genes (*FOXJ1*, *CDHR3*, *MYB* and *CDK1*) unspliced/spliced mRNA read ratios and expression levels projected onto UMAP embedding. Unspliced/spliced mRNA ratios for each cell, colored by major ciliated subsets (the left panel); key genes with color-coded by upspliced/spliced mRNA ratios projected onto UMAP embedding (the middle panel); key genes expression levels projected onto UMAP embedding (the right panel). **g** Histograms showing ECE treatment specific ciliated cell percentage from six groups. PAGA: Partition- based graph abstraction

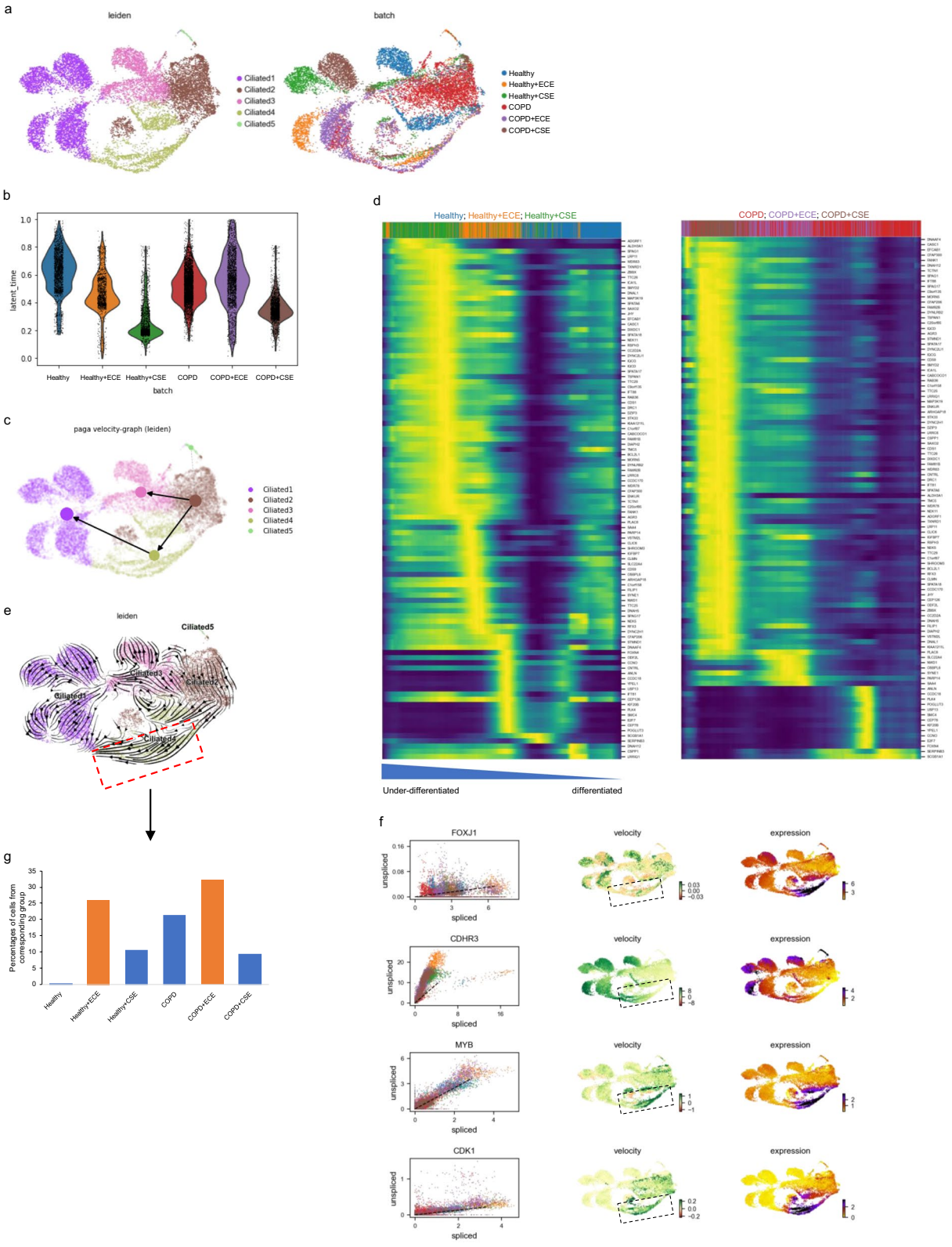

Fig. 2 (See legend on previous page.)

cultures (Fig. 2d). Similarly, pre-ciliated gene *RXF3* and *DNAH5* were highly expressed in CSE treatment group, with medium levels in the ECE treatment group and were barely detected in the non-treatment group in healthy nonsmoker ALI cultures (Fig. 2d).

Notably, RNA velocity analysis showed that ECE treatment specifically enriched the ciliated4 cluster (Fig. 2e), which highly expressed two early ciliogenesis markers (*MYB* and *CDK1*) [17, 18] at the upstream of RNA velocity inferred path. Velocity signals of these two markers were gradually decreased towards the end of the path, showing gradually increasing velocity signals marked by *CDHR3* that represented mature ciliated cells (Fig. 2f highlighted in black-dash box). Moreover, the majority (57.9%) of these ECE specific ciliated cell populations (the red-dash box in Fig. 2e) was from healthy (25.9%) and COPD (32%) treated by ECE (Fig. 2g). These results indicate that the ciliated4 cluster represents a unique feature of ECE treatment on ciliated cells.

Cell-to-cell communications within and between clusters in ALI-cultured HBE cells from healthy nonsmokers and COPD smokers treated by ECE or CSE

Cell-to-cell communications play essential roles in airway epithelial cell differentiation. Next, we used CellChat [19] to investigate differences in cell-to-cell communications in ALI-cultured HBE cells from healthy nonsmokers or COPD smokers treated by ECE or CSE. Based on CellChat database, we characterized cell- to-cell communication frequencies among cell types identified in multiple pathways. Notch signaling is essential for airway epithelial cell differentiation [20]. For healthy nonsmoker ALI cultures, we found that Notch signaling strength was upregulated in ciliated4 upon ECE treatment but not upon CSE treatment (Fig. 3a and B). There was a universal decrease in DESMOSOME pathway upon ECE or CSE treatment (Fig. 3a and B). For ciliated3 cluster, OCLN pathway was dramatically decreased upon ECE or CSE treatment (Fig. 3a and B). The club cell cluster also exhibited decreased EPHB signals upon ECE or CSE treatment (Fig. 3a and B). For COPD smoker ALI cultures, we also observed increased Notch signaling strength in ciliated4 cluster upon ECE or CSE treatment (Fig. 3c and D). There was a universal increase in DESMOSOME signal strength upon ECE or CSE treatment. We then analyzed expression of Notch signaling components. Expression levels of *NOTCH1/2/3* were all increased upon ECE treatment in multiple cell populations in healthy nonsmoker ALI cultures (Fig. 3e). Interestingly, *JAG1* was upregulated in ciliated4 cluster upon ECE or CSE treatment in healthy nonsmoker ALI cultures (Fig. 3e). These results indicate that abnormal activation of Notch pathway may contribute to the dysregulation of ciliated cells caused by ECE or CSE treatment. In addition, we found that COPD smoker non-treatment ALI cultures already exhibited upregulated Notch signaling compared with healthy nonsmoker non-treatment (Fig. 3e and F).

For the ciliated4 cluster, COPD smoker ALI cultures treated by ECE or CSE maintained high *JAG1* levels, significantly higher than non-treatment healthy nonsmokers (Fig. 3e, f and h). Altogether, these results suggest that abnormal activation of Notch pathway signaling is a common feature in HBE cells from healthy nonsmokers and COPD smokers upon treatment with ECE or CSE.

Consistency of identifying similar cell populations between our scRNA-Seq data and published scRNA-Seq data (PRJEB44878) of HBE cells in ALI cultures

To examine whether HBE cell populations identified in our scRNA-Seq data is similar to those of published scRNA-Seq data generated using similar CS in silico analysis, we downloaded scRNA-seq data from a previous study, which used similar smoke exposure strategy (for the smoke exposure upon differentiation, small airway epithelial cells (SAECs) were exposed to whole CS of 3R4F reference cigarettes three times a week during the differentiation phase (28 days) beginning on day 0 (= day of air-lift)) [21]. We annotated our scRNA-seq clusters using the published markers (PMID: 34299265; PRJEB44878) and performed integration analysis. We found that the cell distribution between our data and the public data (PRJEB44878) is highly similar (supplementary figure S3a). The transcriptomes of identified cell types between our data and PRJEB44878 also showed highly correlated (supplementary figure S3b). In addition, the expression patterns of the key markers for clusters were highly similar between our data and these published data (supplementary figure S3c). These results suggest that our data recapture the consistent smoke effects on HBE cells with previous published study.

ECE exposure leads to hypoplasia of acetylated α-tubulin$^+$ ciliated cells and SCGB1A1$^+$ club cells

Next, we examined the effect of ECE on bronchial epithelial cell remodeling by immunostaining. The relative number of acetylated α-tubulin$^+$ ciliated cells was significantly reduced in ECE-treated ALI cultures compared with controls in healthy nonsmokers or COPD smokers, similar to those observed in CSE-treated samples (Fig. 4a, b, d and e). Interestingly, we did not observe significant changes in numbers of MUC5AC$^+$ goblet cells upon ECE treatment in healthy nonsmokers or in COPD smokers (Fig. 4a, c, d, f), although CSE-treated samples exhibited significantly increased numbers of MUC5AC$^+$ goblet cells (Fig. 4a, c, d, f).

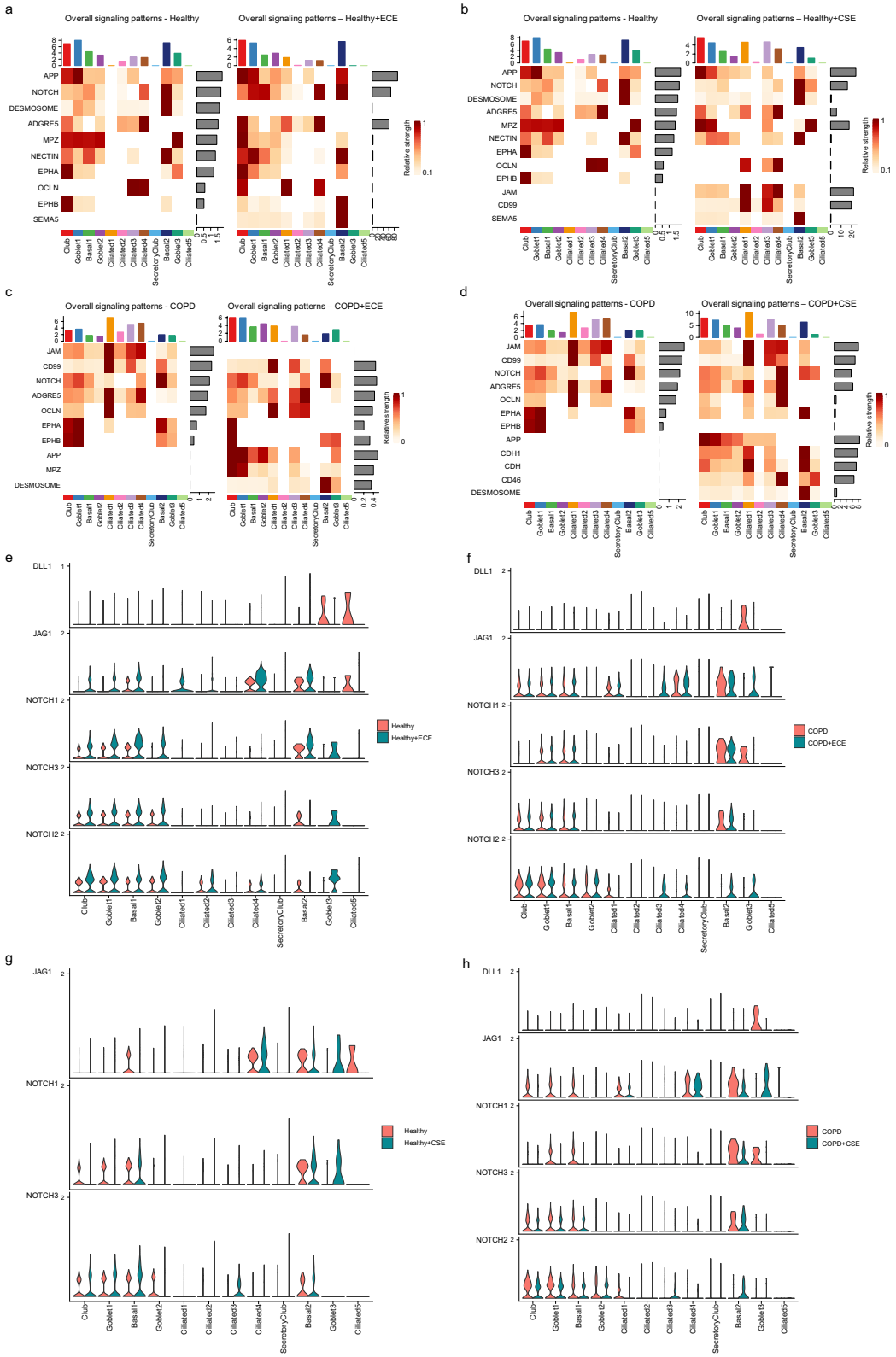

Fig. 3 Cell–cell communication analysis of HBE cells. **a**-**d** CellChat analysis showing comparisons of cell–cell communication pathways for each cell cluster **a** between healthy and healthy + ECE; **b** between healthy and healthy + CSE; **c** between COPD and COPD + ECE; **d** between COPD and COPD + CSE. **e–h** Expression levels of Notch signaling components including *DLL1*, *JAG1*, *NOTCH1*, *NOTCH2* and *NOTCH3*in each cell cluster **e** between healthy and healthy + ECE; **f** between COPD and COPD + ECE; **g** healthy and healthy + CSE; **h** between COPD and COPD + CSE

SCGB1A1$^+$ secretory cells locate in both human bronchi and bronchioles [22]. ECE- treated or CSE-treated ALI cultures exhibited a similar significant decrease in numbers of *SCGB1A1*$^+$secretory cells compared with controls in healthy nonsmokers (Fig. 4g and h). Next, we examined bronchial epithelial cell proliferation by immunostaining for Ki67, a cell cycle marker, and found that ECE exposure displayed no obvious differences in numbers of proliferating basal cells or pan-epithelial cells from healthy nonsmokers or COPD smokers (supplementary figure S4a-d andS5a-d). Altogether, these data indicate that ECE specifically affect airway epithelial cell differentiation but not proliferation in healthy nonsmokers and COPD patients.

ECE exposure leads to decreased HBE cell barrier integrity in ALI cultures

To test the effect of ECE exposure on epithelial barrier function, we examined changes in transepithelial electrical resistance (TEER) of HBE cells in ALI culutres. CSE exposure has been reported to reduce bronchial epithelial barrier integrity in ALI cultures. Interestingly, ECE-treated HBE cells also exhibited compromised epithelial barrier integrity as evidenced by decreased TEER in healthy nonsmokers compared with controls, similar to those found in CSE-treated ALI cultures (supplementary figure S6a). Similarly, ECE-treated HBE cells also displayed impaired epithelial barrier function in COPD smokers compared with controls, similar to those found in CSE-treated ALI cultures (supplementary figure S6b). These results suggest that ECE exposure may disrupt bronchial epithelial cell barrier function.

ECE exposure leads to cilia shortening in HBE cells from healthy nonsmokers and COPD smokers

CSE exposure has been shown to cause injury to airway cilia [23]. ECE treatment also led to reduced cilia length in healthy nonsmokers or COPD smokers compared with controls, similar to those found in CSE-treated ALI cultures (Fig. 5a–f). FOXJ1 is essential for ciliogenesis in the airways [23–25]. ECE-treated ALI cultures exhibited decreased *FOXJ1* mRNA levels compared with controls in healthy nonsmokers or COPD smokers, which was also observed in the CSE treatment group (Fig. 5g and h). Smoking has been reported to induce pulmonary epithelial cell injury. We then examined changes in levels of SCGB1A1, a marker of airway epithelial injury in ALI cultures. ECE-treated ALI cultures exhibited significantly reduced SCGB1A1 protein levels in supernatants compared with controls in healthy nonsmokers and COPD smokers, similar to those observed in the CSE treatment group (Fig. 5i, j). These results indicate that ECE exposure compromises cilia formation and induces epithelial cell injury during HBE cell differentiation.

Notch signaling as a mediator of ECE exposure-caused ciliated cell remodeling and cilia shortening

Since Notch signaling activation is essential for airway epithelial cells differentiation in mice and humans [20, 26, 27], and Notch signaling strength was upregulated in ciliated cell subpopulations upon ECE treatment (Fig. 3a, c), we examined whether inhibition of Notch signaling could ameliorate ciliated cell remodeling caused by ECE exposure. We used DATP, a γ-secretase inhibitor that prevents cleavage of the intracellular domain of Notch receptors

(See figure on next page.)

Fig. 4 ECE exposure causes reduced numbers of ciliated cells and club cells from healthy nonsmokers or COPD smokers. **a** Immunostaining for MUC5AC (red), acetylated α-tubulin (green) and DAPI staining (blue) in HBE cells from healthy nonsmokers at the ALI after 9 day DMEM/F-12 medium (n = 5), ECE (n = 5) or CSE (n = 5) treatment. **b** Quantification of the relative number of acetylated α-tubulin$^+$ cells in HBE cells from healthy nonsmokers at the ALI after 9 day DMEM/F-12 medium (n = 5), ECE (n = 5) or CSE (n = 5) treatment. 4752, 3392 and 1701 acetylated α-tubulin$^+$ cells were analyzed for controls, ECE and CSE treatment, respectively. **c** Quantification of the relative number of MUC5AC$^+$cellsinHBE cells from healthy nonsmokers at the ALI after 9 day DMEM/F-12 medium (n = 5), ECE (n = 5) or CSE (n = 5) treatment.1604, 2304 and 3592 MUC5AC$^+$ cells were analyzed for controls, ECE and CSE treatment, respectively. **d** Immunostaining for MUC5AC (red), acetylated α-tubulin (green) and DAPI staining (blue) in HBE cells from COPD smokers at the ALI after 9 day DMEM/F-12 medium (n = 5), ECE (n = 5) or CSE (n = 5) treatment. **e** Quantification of the relative number of acetylated α-tubulin$^+$ cells in HBE cells from COPD smokers at the ALI after 9 day DMEM/F-12 medium (n = 5), ECE (n = 5) or CSE (n = 5) treatment.3504, 2260 and 1296 acetylated α-tubulin$^+$ cells were analyzed for controls, ECE and CSE treatment, respectively. **f** Quantification of the relative number of MUC5AC$^+$cells in HBE cells from COPD smokers at the ALI after 9 day DMEM/F-12 medium (n = 5), ECE (n = 5) or CSE (n = 5) treatment. 1952, 2702 and 3552 MUC5AC$^+$ cells were analyzed for controls, ECE and CSE treatment, respectively. **g** Immunostaining for SCGB1A1 (green) and DAPI staining (blue) in HBE cells from healthy nonsmokers at the ALI after 9 day DMEM/F-12 medium. (n = 5), ECE (n = 5) or CSE (n = 5) treatment. **h** Quantification of the relative number of SCGB1A1$^+$ cells in HBE cells from healthy nonsmokers at the ALI after 9 day DMEM/F-12 medium (n = 5), ECE (n = 5) or CSE (n = 5) treatment. 8752, 5592 and 4684 SCGB1A1$^+$cells were analyzed for controls, ECE and CSE treatment, respectively. Scale bars: 100 μm. Unpaired Student's *t*-test, mean ± s.d

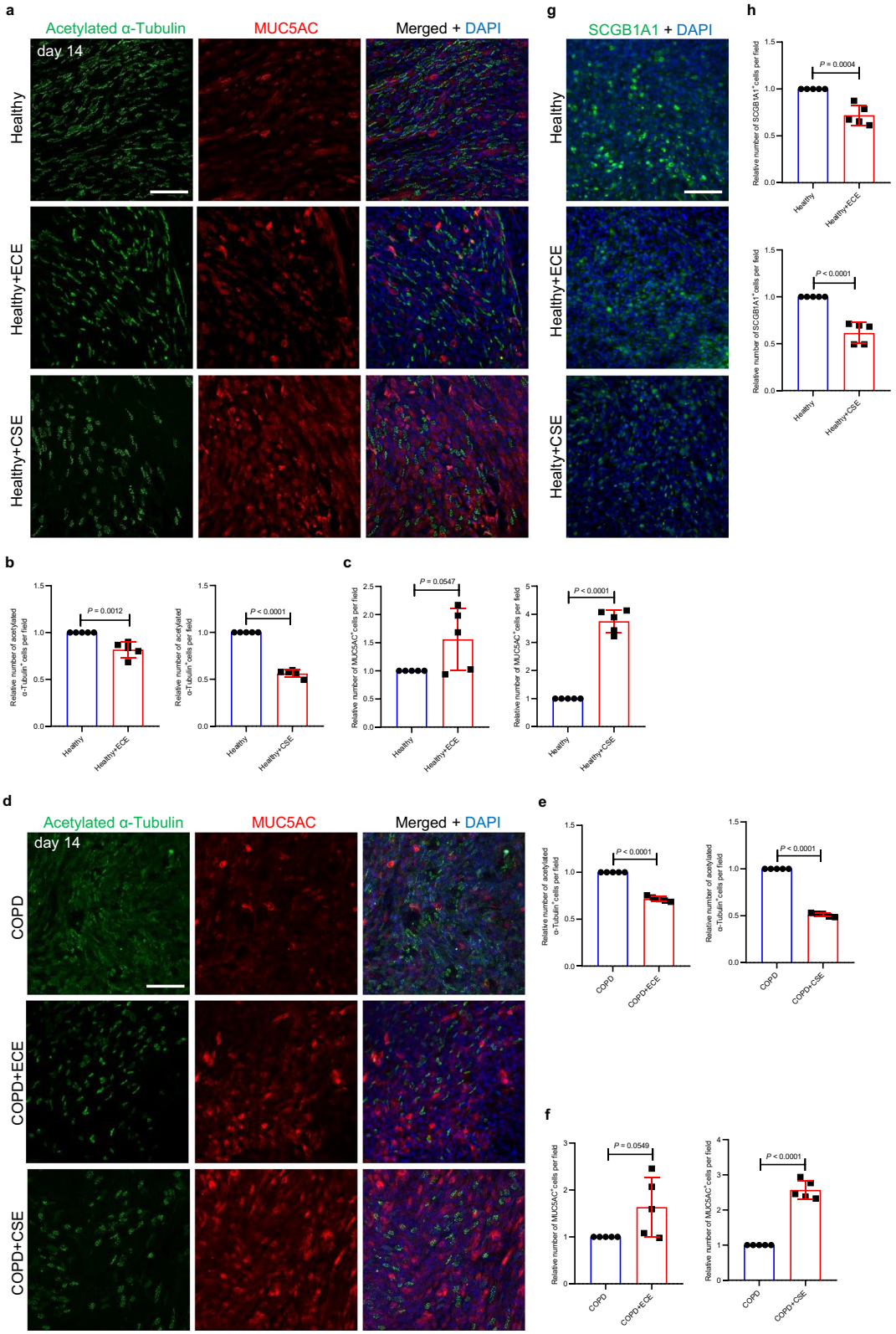

Fig. 4 (See legend on previous page.)

driving the downstream transcriptional effects of Notch signaling to treat HBE cells. A 10 μM DAPT treatment partially restored ECE treatment-induced ciliated cell differentiation defects in ALI cultures in healthy nonsmokers or COPD smokers, similar to those observed in the CSE treatment groups (Fig. 6a, b, c, e and f). As expected, CSE treatment-induced hyperplasia of $MUC5AC^+$ goblet cells was also partially rescued after DAPT treatment in healthy nonsmokers or COPD smokers (Fig. 6d and g) [27]. Inhibition of Notch signaling has recently been reported to enhance ciliogenesis in cultured human nasal epithelial cells [28]. Next, we examined whether inhibition of Notch signaling could suppress ECE exposure-induced cilia shortening in HBE cells. 10 μM DAPT treatment attenuated ECE treatment-induced cilia shortening in ALI cultures in healthy nonsmokers or COPD smokers, similar to those observed in the CSE treatment groups (Fig. 7a–d).

Next, we examined the effect of DAPT at a lower dose on ECE or CSE-induced HBE cell differentiation (supplementary figure S7 and supplementary figure S8). A 2.5 μM DAPT treatment also partially restored ECE treatment-induced ciliated cell differentiation defects in ALI cultures in healthy nonsmokers (supplementary figure S7a-c) or COPD smokers (supplementary figure S7d, e), similar to those observed in the CSE treatment groups (supplementary figure S8a-e). CSE treatment-induced $MUC5AC^+$ goblet cell hyperplasia was also partially restored after 2.5 μM DAPT treatment in healthy nonsmokers (supplementary figure S8b, c) or COPD smokers (supplementary figure S8d, e). We have also tested the effect of DBZ, another Notch singling inhibitor, on ECE or CSE-induced HBE cell differentiation (supplementary figure S9 and supplementary figure S10). A 0.5 μM DBZ treatment could also partially restore ECE treatment-induced ciliated cell differentiation defects in ALI cultures in healthy nonsmokers (supplementary figure S9a-c) or COPD smokers (supplementary figure S9d, e), similar to those observed in the CSE treatment groups (supplementary figure S10a-e). CSE treatment-induced $MUC5AC^+$ goblet cell hyperplasia was also partially restored after 0.5 M DBZ treatment in healthy nonsmokers (supplementary figure S10b, c) or COPD smokers (supplementary figure S10d, e). These results indicate that Notch signaling activation in ECE or CSE- exposure ALI cultures partially accounts for HBE cell remodeling and injury phenotypes.

SCGB1A1 levels are decreased in serum and sputum of e-cigarette users

Decreased levels of SCGB1A1has been reported to be associated with airway epithelial injury and pulmonary diseases, including COPD and COVID-19. We collected serum and sputum from healthy nonsmokers, e-cigarette users, cigarette smokers and COPD smokers (Table S3). Both e-cigarette users exhibited significantly reduced SCGB1A1 levels in serum or sputum compared with healthy nonsmoker, similar to those observed in tobacco smokers (Fig. 8a, b). Next, we examined MUC5AC levels. E-cigarette users exhibited no significant difference in MUC5AC levels compared with healthy nonsmokers in serum or sputum (Fig. 8c and d). Cigarette smokers exhibited significantly increased MUC5AC levels in both serum and sputum compared with healthy nonsmokers or e-cigarette users (Fig. 8c and d).

Interestingly, COPD smokers exhibited highest MUC5AC levels in serum in these four groups (Fig. 8c). These in vivo results suggest that airway club cells are one of primary injury targets by e-cigarette use.

Discussion

Tobacco smoking causes airway remodeling and alveoli disruption in the lungs. Airway remodeling is one of the main causes of airflow obstruction in cigarette smokers with COPD [29]. Cilia injury can lead to impaired mucociliary clearance and formation of a mucus plug, which are associated with airflow limitation [30]. A nicotine-intake alternative to tobacco, such as e-cigarette

(See figure on next page.)

Fig. 5 ECE exposure leads to cilia shortening in HBE cells from healthy nonsmokers or COPD smokers. **a** Hematoxylin and eosin staining for ALI culture sections of HBE cells from healthy nonsmokers after 9 day DMEM/F-12 medium (n = 5), ECE (n = 5) or CSE (n = 5) treatment. **b** Immunostaining for acetylated α- tubulin (green) and DAPI staining (blue)for ALI culture sections of HBE cells from healthy nonsmokers after 9 day DMEM/F-12 medium (n = 5), ECE (n = 5) or CSE (n = 5) treatment. **c** Quantification of cilia length in HBE cells from healthy. Nonsmokers at the ALI after 9 day DMEM/F-12 medium (n = 5), ECE (n = 5) or CSE (n = 5) treatment. **d** Hematoxylin and eosin staining for ALI culture sections of HBE cells from COPD smokers after 9 day DMEM/F-12 medium (n = 5), ECE (n = 5) or CSE (n = 5) treatment. **e** Immunostaining for acetylated α-tubulin (green) and DAPI staining (blue) for ALI culture sections of HBE cells from COPD smokers after 9day DMEM/F-12 medium (n = 5), ECE (n = 5) or CSE (n = 5) treatment. **f** Quantification of cilia length in HBE cells from COPD smokers at the ALI after 9 day DMEM/F-12 medium (n = 5), ECE (n = 5) or CSE (n = 5) treatment. **g, h** RT- qPCR analysis of mRNA levels of *FOXJ1* in HBE cells from **g** healthy nonsmokers or **h** COPD smokers at the ALI after 9 day DMEM/F-12 medium (n = 3), ECE (n = 3) or CSE (n = 3) treatment. **i, j** ELISA measurements of SCGB1A1 levels in supernatant of HBE cells from **i** healthy nonsmokers or **j** COPD smokers at the ALI after 9 day DMEM/F-12 medium (n = 3), ECE (n = 3) or CSE (n = 3) treatment. Scale bars: 50 μm. Unpaired Student's *t*-test, mean ± s.d

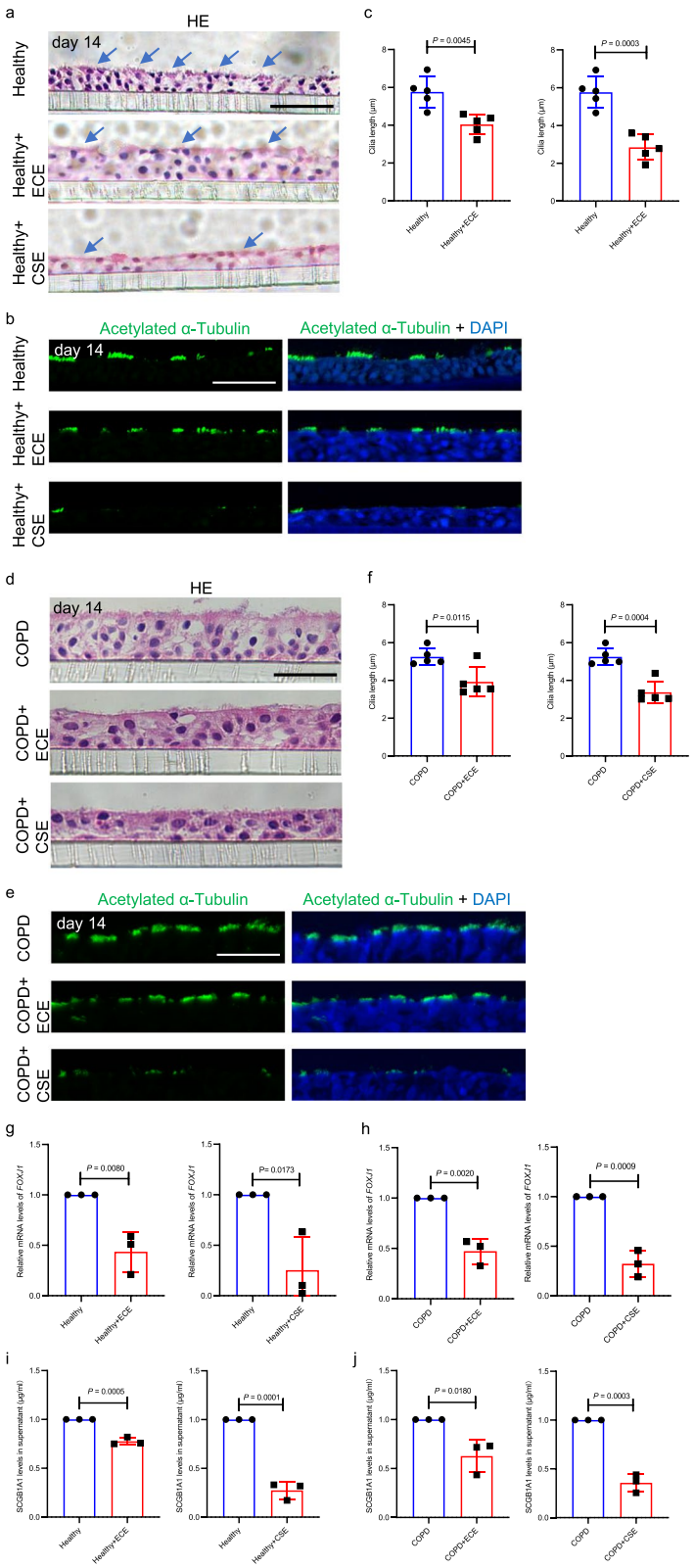

Fig. 5 (See legend on previous page.)

has come to the market and increasingly used by young people. Given the unclear health effects of e-cigarettes, it is important to understand its contributions to airway remodeling and injury. In this study, we compared the effects of ECE with those of CSE on ALI-cultured HBE cells from healthy nonsmokers or COPD smokers at an equal nicotine concentration of 0.02 mg/ml. We found that both ECE and CSE treatment led to a reduction of ciliated cells and club cells, and cilia length from healthy nonsmokers both COPD smokers. Although previous studies show that ECE treatment leads to downregulation of cilia- related genes, and flavoring chemicals such as diacetyl and 2,3-pentanedione found in e-cigarette treatment also decreases expression of genes related to ciliogenesis and reduces number of ciliated cells [10, 11], our study showed that ECE treatment led to changes in differentiation of some of ciliated cell subtypes but not all ciliated cell subtypes. For example, ECE treatment did not lead to obvious changes in differentiation of the ciliated4 cluster that expressed *PLK4*, *DEUP1*, *FOXN4* and *CENPJ.* Since we treated HBE cells using ECE or CSE with one nicotine concentration in this study, it remains necessary to compare the effects of ECE on HBE cells with those elicited by CSE at other concentrations.

Cigarette smoking is associated with shortened cilia in human airways [31]. CSE exposure has been reported to suppress cilia growth in HBE cells in ALI cultures [23]. Here, we show for the first time that ECE exposure also reduces cilia length in HBE cells from healthy nonsmokers or COPD smokers, similar to the phenotypes caused by CSE treatment. Since nicotine is present in both CSE and ECE, it is possible that nicotine is one of these components that can induce cilia shortening. It will be worth examining whether nicotine treatment alone could also cause changes in cilia length in bronchial epithelial cells. ECE contains distinct components such as propylene glycol, glycerol and flavors. It would be interesting to test their effects on cilia formation.

A study has reported that CSE treatment causes no significant changes in numbers of acetylated α-tubulin$^+$ ciliated cells in ALI cultures of healthy donors or COPD smokers [27], which is different from our observation. This may be due to a different CSE concentration treatment or a later stage CSE treatment in their experiments.

They exposed HBE cell ALI cultures of healthy donors or COPD smokers to 2.5% CSE from ALI day 28 to ALI day 35, and analyzed samples at ALI day 35. It is possible that this CSE concentration is lower than that with a nicotine concentration of 0.02 mg/ml used in our studies. Another possibility is that CSE exposure can compromises ciliated cell differentiation at an earlier time frame such as from ALI day 5 to day 14 in our study.

Acute exposure to high-wattage e-cigarettes has been reported to induce increased SCGB1A1 levels in serum, which reflects lower airway injury [32]. However, e- cigarette users exhibited significantly reduced SCGB1A1 levels in serum compared with healthy nonsmokers, similar to those found in HBE cell supernatant in our study. It is possible that short-term exposure to e-cigarette vaper caused acute injury to airway epithelial cell to release SCGB1A1 into the plasma, which leads to increased SCGB1A1 levels in serum. In long-term e-cigarette users, numbers of SCGB1A1$^+$ club cell may be significantly reduced and/or SCGB1A1 expression is decreased, which ultimately leads to decreased SCGB1A1 levels. It remains worth examining changes in numbers of club cells by analyzing lung tissues of long-term e-cigarette users. Another study reports that e-cigarette users exhibited no significant changes in SCGB1A1 levels in plasma compared to healthy subjects who have never used any tobacco products [33]. However, e-cigarette, or vaping, product use-associated lung injury (EVALI) subjects display significantly decreased SCGB1A1 levels in plasma than non-users [34]. It is thus possible that SCGB1A1 is a marker of airway epithelial cell injury for long-term or heavy e-cigarette users.

The NOTCH signaling includes several ligands and receptors. It would be interesting to test which ligand(s) and receptor(s) are main mediators of ECE-induced changes in HBE cell differentiation and cilia injury by using gene overexpression or knockout.

(See figure on next page.)

Fig. 6 Notch signaling functions as mediators of ECE treatment-induced remodeling of HBE cells from in healthy nonsmokers or COPD smokers. **a** Timeline for ECE or CSE and DAPT administration. **b** Immunostaining for acetylatedα-tubulin (green), MUC5AC (red) and DAPI staining (blue) in HBE cells from healthy nonsmokers at the ALI after 16 day DMEM/F-12 medium (n = 3), ECE (n = 3) or CSE (n = 3) treatment, or 16 day ECE and 7 day 10 μM DAPT (n = 3), or 16 day CSE and 7 day 10 μM DAPT (n = 3) treatment. **c** Quantification of the relative number of acetylated α-tubulin$^+$ cells. **d** Quantification of the relative number of MUC5AC$^+$ cells. **e** Immunostaining for acetylated α-tubulin (green), MUC5AC (red) and DAPI staining (blue) in HBE cells from COPD smokers at the ALI after 16 day DMEM/F-12 medium (n = 3), ECE (n = 3) or CSE (n = 3) treatment, or 16 day ECE and 7 day 10 μM DAPT (n = 3), or 16 day CSE and 7 day 10 μM DAPT (n = 3) treatment. **f** Quantification of the relative number of acetylated α-tubulin$^+$ cells. **g** Quantification of the relative number of MUC5AC$^+$cells. Scale bars: 100 μm. One- way ANOVA with Tukey's multiple comparison test for comparisons among three groups and Unpaired Student's *t*-test for comparisons between two groups, mean ± s.d

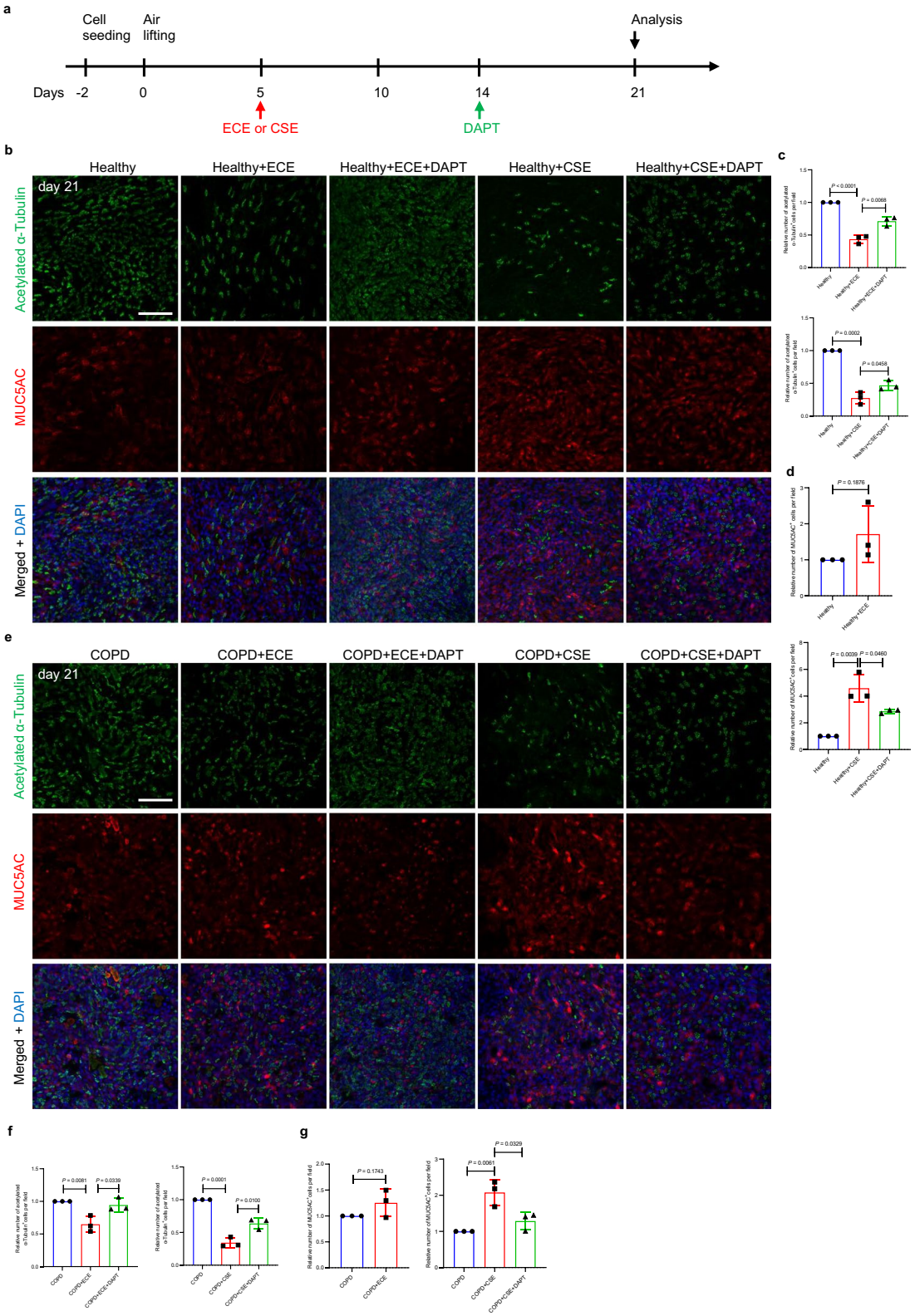

Fig. 6 (See legend on previous page.)

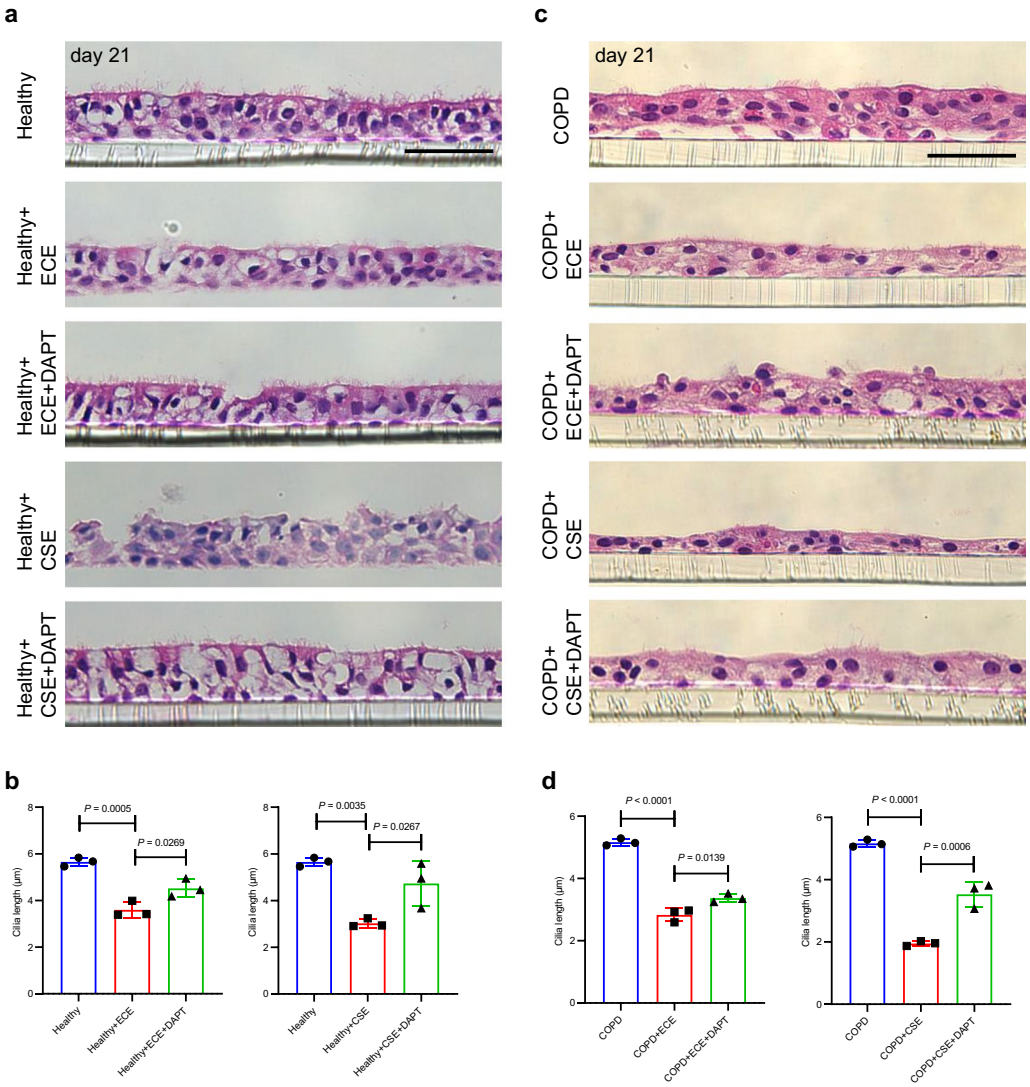

Fig. 7 Notch signaling inhibition partially rescues cilia shortening and mucus hypersecretion induced by ECE treatment in HBE cells from healthy nonsmokers or COPD smokers. **a** Hematoxylin and eosin staining for ALI culture sections of HBE cells from healthy nonsmokers at the ALI after 16F day DMEM/F-12 medium (n = 3), CSE (n = 3) or ECE (n = 3) treatment, or 16 day CSE and 7 day 10 μM DAPT (n = 3), or 16 day ECE and 7 day 10 μM DAPT (n = 3) treatment. **b** Quantification of cilia length in HBE cells. **c** Hematoxylin and eosin staining for ALI culture sections of HBE cells from COPD smokers at the ALI after 16 day DMEM/F-12 medium (n = 3), CSE (n = 3) or ECE (n = 3) treatment, or 16 day CSE and 7 day 10 μM DAPT (n = 3), or 16 day ECE and 7 day 10 μM DAPT (n = 3) treatment. **d** Quantification of cilia length in HBE cells. Scale bars: 50 μm. One- way ANOVA with Tukey's multiple comparison test, mean ± s.d

Since several other pathways including Hedgehog and Wnt have been reported to regulate airway epithelial cell differentiation [25, 35–37], it would be worth examining whether ECE exposure causes changes in them as well.

We exposed HBE cells cultured at ALI to ECE or CSE in the basal medium, which is not fully modeling the in vivo situation where the airway epithelium's apical surface is exposed to vapor. Our study is more likely to reflect effects that e-cigarette or tobacco products have on the airway epithelium through circulation. Thus, it would be worth testing the effect of apical exposure of e-cigarette or tobacco vapor on HBE cells.

Limitation of this study

In this study, we adjust nicotine concentrations to comparable levels for exposures, which leads to different concentrations of other components between ECE and CSE and may cause different responses of HBE cells to them. For example, the concentration of propylene glycol (PG), glycerol (Gly), menthol racemic and ethyl alcohol

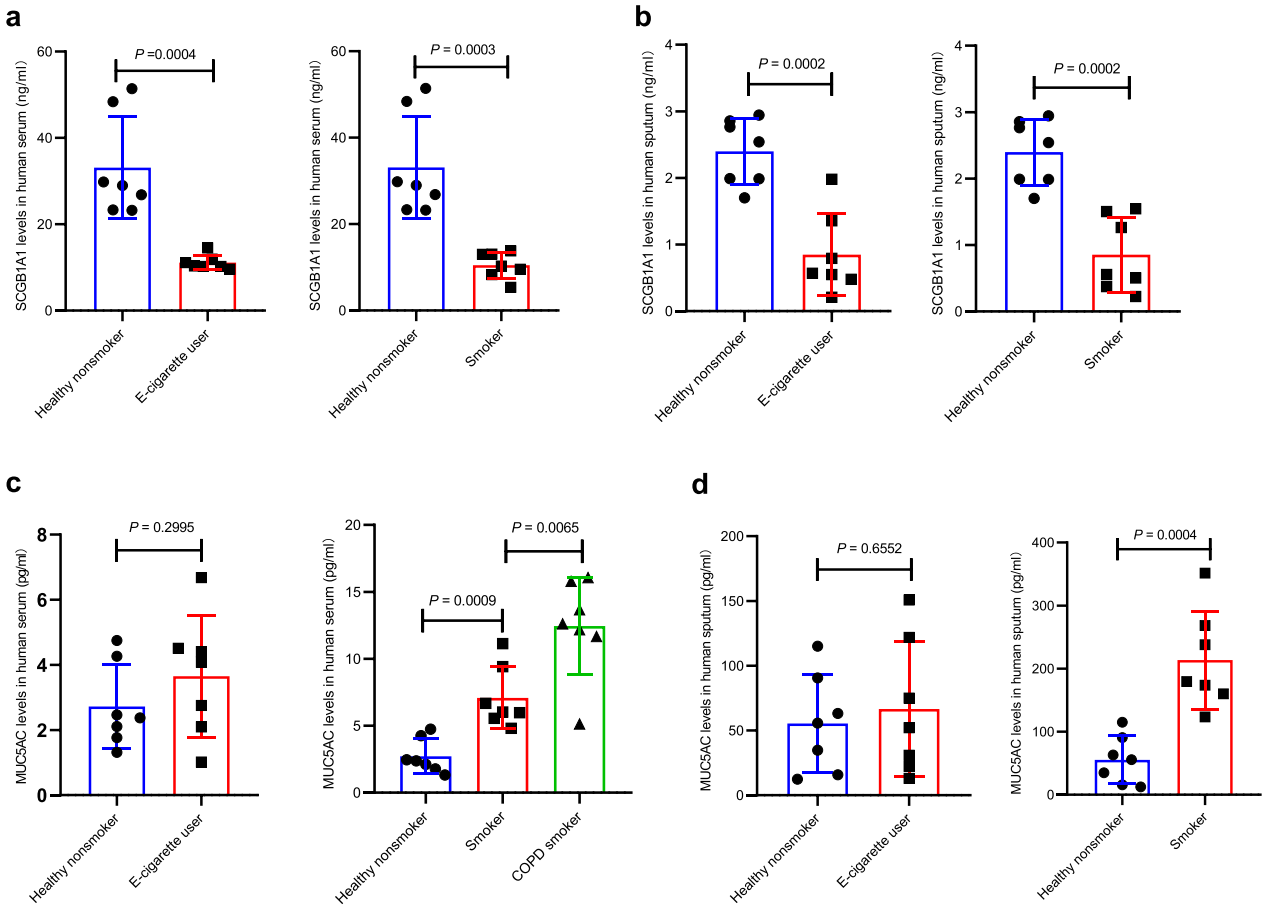

Fig. 8 SCGB1A1 levels are decreased in the serum and sputum of E- cigarette users. **a** ELISA measurements of SCGB1A1 levels in serum of healthy nonsmokers, e-cigarette users and tobacco smokers. **b** ELISA measurements of SCGB1A1 levels in sputum of healthy nonsmokers, e-cigarette users and tobacco smokers. **c** ELISA measurements of MUC5AC levels in serum of healthy nonsmokers, e-cigarette users, tobacco smokers and COPD smokers. **d** ELISA measurements of MUC5AC levels in sputum of healthy nonsmoker, e-cigarette users and tobacco smokers. Unpaired Student's *t*-test, mean ± s.d

is 0.117 mg.mL^{-1}, 0.178 mg.mL^{-1}, 0.006 mg.mL^{-1} and 0.013 mg.mL^{-1}in ECE, respectively, which is less than the detection limit of GC–MS in CSE. However, the concentration of glycerol triacetate is 0.006 mg.mL^{-1}, which is less than the detection limit of GC–MS in ECE. Although, PG and glycerol can slightly inhibit proliferation of human small airway epithelial cells at the concentration of 10 mg.mL^{-1} and 20 mg.mL^{-1}, respectively [38], much higher than those we used for HBE cell treatments in this study, it is possible that differences in these combined components between ECE and CSE cause different responses of HBE cells to them. It remains worth examining effects of these component differences on HBE cell differentiation and injury.

We use of menthol-flavored e-cigarettes as the e-cigarette exposure group. It is possible that menthol itself causes these effects on HBE cells. There is need to examine how other flavored e-cigarettes such as tobacco-flavored ones affect HBE cells.

In this study, healthy non-smokers we recruited were younger that COPD patients (66.2 years old in average versus 74.6 years old in average). It will be interesting and necessary to collect healthy nonsmokers with more similar ages to COPD smokers, and compare the effect of ECE or CSE on HBE cell remodeling and injury between healthy nonsmokers and COPD smokers in future studies. In addition, we have not collected HBE cell samples from female COPD patients at this moment. In healthy nonsmokers, we obtained HBE cells from 3 males and 2 females. It will be necessary to also collect HBE cells from female COPD patients to test whether the effect of ECE or CSE on HBE cell remodeling and injury is similar compared with those of male COPD patients in future studies.

Supplementary Information

The online version contains supplementary material available at https://doi.org/10.1186/s12931-024-02962-4.

Additional file 1: Figure S1: Marker genes for key HBE cell types. Figure S2: Expression levels of key marker genes in HBE cell populations. Figure S3: Consistency of identifying similar cell populations between our scRNA-Seq data and published scRNA-Seq data (PRJEB44878) of HBE cells in ALI cultures. Figure S4: ECE exposure leads to no significant differences in proliferation of HBE cells or basal cells from healthy nonsmokers. Figure S5: ECE exposure causes no significant differences in proliferation of HBE cells or basal cells from COPD smokers. Figure S6: ECE exposure leads to reduced transepithelial electrical resistance (TEER) of HBE cells from healthy nonsmokers and COPD smokers. Figure S7: Low dose DAPT treatment partially restores ECE treatment-induced remodeling of HBE cells from healthy nonsmokers and COPD smokers. Figure S8: Low dose DAPT treatment partially restores CSE treatment-induced remodeling of HBE cells from healthy nonsmokers and COPD smokers. Figure S9: DBZ treatment partially restores ECE treatment-induced remodelling of HBE cells from healthy nonsmokers and COPD smokers. Figure S10: DBZ treatment partially restores CSE treatment-induced remodeling of HBE cells from healthy nonsmokers and COPD smokers. Table S1: Healthy nonsmoker and COPD patient information for Figure 1 to Figure 7. Table S2: The analysis of the main components in ECE and CSE used for HBE cells treatment in this study by GC-MS. Table S3: Healthy nonsmoker, E-cigarette user, cigarette smoker and COPD patient information for Figure 8.

Acknowledgements
We thank Shiyue Li and Lei Wang for discussions and assistance.

Author contributions
W.Y. conceived the project and designed the experiments; W.C., L.C. and R.Y. performed experiments and data analysis; J.L., Z.W. and Z.Z. performed data analysis; W.Y. and J.L. wrote the manuscript; P.R., G.H. W.Z. and Y.Z. provided clinical guidance; X. J. provided infrastructure; W.Y., P.R. and T.Z. supervised the whole study and approved this version before submission.

Funding
This study was supported by the grants from the National Natural Science Foundation of China (81970019, 82370148), R&D Program of Guangzhou Laboratory (GZNL2024A02005, GZNL2023A02003, SRPG22-021, SRPG22-016, YW-JCYJ0505), Guangzhou Municipal Science and Technology Bureau, Guangzhou Key Research and Development Program (2024B03J0046),Supported by the grant of State Key Laboratory of Respiratory Disease (SKLRD-Z-202307); Plan on enhancing scientific research in GMU (02-410-2302244XM), Open Research Fund of State Key Laboratory of Genetic Engineering, Fudan University (No. SKLGE-2305), the Open Project of the State Key Laboratory of Respiratory Disease (SKLRD-OP-202110), the National Natural Science Foundation of China (31501169), Guangdong Basic and Applied Basic Research Foundation (2024A1515012968, 2022A1515011058), Scientific Research Project of Education Department of Guangdong Province (2023ZDZX2042, 2021KTSCX087), Tertiary Education Scientific research project of Guangzhou Municipal Education Bureau (Yangcheng Scholar, 202235405), the open research funds from the Affiliated Qingyuan Hospital (Qingyuan People's Hospital), Guangzhou Medical University (202201-306) and the open research funds from GMU-GIBH Joint School of Life Sciences, Guangzhou Medical University.

Data availability
The authors declare that all data supporting the findings of this study are available within the article and its supplementary information files or from the corresponding author upon reasonable request.

Declarations

Consent for publication
Not applicable.

Competing interests
The authors declare no competing interests. At the time of the research, Zehong Wu and Xingtao Jiang were employees of RELX Science Center, Shenzhen RELX Tech.

Author details
[1]State Key Laboratory of Respiratory Disease, National Clinical Research Center for Respiratory Disease, Guangzhou Institute of Respiratory Health, The First Affiliated Hospital of Guangzhou Medical University, Guangzhou, Guangdong 510182, People's Republic of China. [2]Guangzhou National Laboratory, Guangzhou International Bio Island, No. 9 Xing Dao Huan Bei Road, Guangzhou 510005, Guangdong, China. [3]GMU- GIBH Joint School of Life Sciences, Guangzhou Medical University, Guangzhou, China. [4]Key Laboratory of Biological Targeting Diagnosis, Therapy and Rehabilitation of Guangdong Higher Education Institutes, The Fifth Affiliated Hospital of Guangzhou Medical University, Guangzhou, China. [5]RELX Science Center, Shenzhen RELX Tech. Co.,Ltd., Shenzhen, China. [6]Department of Respiratory Medicine, The Third Affiliated Hospital of Guangzhou Medical University, Guangzhou, Guangdong, China. [7]State Key Laboratory of Respiratory Disease, Guangzhou Chest Hospital, Guangzhou, Guangdong, China. [8] State Key Laboratory of Respiratory Disease, Guangzhou Institute of Cancer Research, the Affiliated Cancer Hospital, Guangzhou Medical University, Guangzhou, China. [9]GMU-GIBH Joint School of Life Sciences, The Guangdong-Hong Kong-Macau Joint Laboratory for Cell Fate Regulation and Diseases, State Key Laboratory of Respiratory Disease, The Affiliated Qingyuan Hospital (Qingyuan People's Hospital), Guangzhou Medical University, Guangzhou, Guangdong, People's Republic of China.

Received: 7 September 2023 Accepted: 26 August 2024
Published online: 28 September 2024

References

1. Reidel B, Radicioni G, Clapp PW, Ford AA, Abdelwahab S, Rebuli ME, et al. E-cigarette use causes a unique innate immune response in the lung, involving increased neutrophilic activation and altered mucin secretion. Am J Respir Crit Care Med. 2018;197:492–501.
2. Ghosh A, Coakley RD, Ghio AJ, Muhlebach MS, Esther CR Jr, Alexis NE, et al. Chronic E-cigarette use increases neutrophil elastase and matrix metalloprotease levels in the lung. Am J Respir Crit Care Med. 2019;200:1392–401.
3. Gellatly S, Pavelka N, Crue T, Schweitzer KS, Day BJ, Min E, et al. Nicotine-Free e-Cigarette Vapor exposure stimulates il6 and mucin production in human primary small airway epithelial cells. J Inflamm Res. 2020;13:175–85.
4. Garcia-Arcos I, Geraghty P, Baumlin N, Campos M, Dabo AJ, Jundi B, et al. Chronic electronic cigarette exposure in mice induces features of COPD in a nicotine- dependent manner. Thorax. 2016;71:1119–29.
5. Madison MC, Landers CT, Gu BH, Chang CY, Tung HY, You R, et al. Electronic cigarettes disrupt lung lipid homeostasis and innate immunity independent of nicotine. J Clin Invest. 2019;129:4290–304.
6. Chung S, Baumlin N, Dennis JS, Moore R, Salathe SF, Whitney PL, et al. Electronic cigarette Vapor with nicotine causes airway mucociliary dysfunction preferentially via TRPA1 receptors. Am J Respir Crit Care Med. 2019;200:1134–45.
7. Tsai M, Song MA, Mcndrew C, Brasky TM, Freudenheim JL, MathéE, et al. Electronic versus combustible cigarette effects on inflammasome component release into human lung. Am J Respir Crit Care Med. 2019;199:922–5.
8. Shen Y, Wolkowicz MJ, Kotova T, Fan L, Timko MP. Transcriptome sequencing reveals e-cigarette vapor and mainstream-smoke from tobacco cigarettes activate different gene expression profiles in human bronchial epithelial cells. Sci Rep. 2016;6:23984.
9. Herr C, Tsitouras K, Niederstraßer J, Backes C, Beisswenger C, Dong L, et al. Cigarette smoke and electronic cigarettes differentially activate bronchial epithelial cells. Respir Res. 2020;21:67.
10. Park HR, Vallarino J, O'Sullivan M, Wirth C, Panganiban RA, Webb G, et al. Electronic cigarette smoke reduces ribosomal protein gene expression to impair protein synthesis in primary human airway epithelial cells. Sci Rep. 2021;11:17517.

11. Park HR, O'Sullivan M, Vallarino J, Shumyatcher M, Himes BE, Park JA, et al. Transcriptomic response of primaryhuman airway epithelial cells toflavoring chemica ls in electronic cigarettes. Sci Rep. 2019;9(1):1400.
12. Martin EM, Clapp PW, Rebuli ME, Pawlak EA, Glista-Baker E, Benowitz NL, et al. E-cigarette use results in suppression of immune and inflammatory-response genes in nasal epithelial cells similar to cigarette smoke. Am J Physiol Lung Cell Mol Physiol. 2016;311:L135–44.
13. Travaglini KJ, Nabhan AN, Penland L, Sinha R, Gillich A, Sit RV, et al. A molecular cell atlas of the human lung from single-cell RNA sequencing. Nature. 2020;587:619–25.
14. Goldfarbmuren KC, Jackson ND, Sajuthi SP, Dyjack N, Li KS, Rios CL, et al. Dissecting the cellular specificity of smoking effects and reconstructing lineages in the human airway epithelium. Nat Commun. 2020;11:2485.
15. Basnet S, Bochkov YA, Brockman-Schneider RA, Kuipers I, Aesif SW, Jackson DJ, et al. CDHR3 asthma-risk genotype affects susceptibility of airway epithelium to rhinovirus C infections. Am J Respir Cell Mol Biol. 2019;61:450–8.
16. Montoro DT, Haber AL, Biton M, Vinarsky V, Lin B, Birket SE, et al. A revised airway epithelial hierarchy includes CFTR-expressing ionocytes. Nature. 2018;560:319–24.
17. Tan FE, Vladar EK, Ma L, Fuentealba LC, Hoh R, Espinoza FH, et al. Myb promotes centriole amplification and later steps of the multiciliogenesis program. Development. 2013;140:4277–86.
18. Vladar EK, Stratton MB, Saal ML, Salazar-De Simone G, Wang X, Wolgemuth D, et al. Cyclin-dependent kinase control of motile ciliogenesis. Elife. 2018;7:e36375.
19. Jin S, Guerrero-Juarez CF, Zhang L, Chang I, Ramos R, Kuan CH, et al. Inference and analysis of cell-cell communication using Cell Chat. Nat Commun. 2021;12:1088.
20. Rock JR, Gao X, Xue Y, Randell SH, Kong YY, Hogan BL. Notch-dependent differentiation of adult airway basal stem cells. Cell Stem Cell. 2011;8:639–48.
21. Wohnhaas CT, Gindele JA, Kiechle T, Shen Y, Leparc GG, Stierstorfer B, et al. Cigarette smoke specifically affects small airway epithelial cell populations and triggers the expansion of inflammatory and squamous differentiation associated basal cells. Int J Mol Sci. 2021;22:7646.
22. Okuda K, Chen G, Subramani DB, Wolf M, Gilmore RC, Kato T, et al. Localization of secretory mucins MUC5AC and MUC5B in normal/healthy human airways. Am J Respir Crit Care Med. 2019;199:715–27.
23. Brekman A, Walters MS, Tilley AE, Crystal RG. FOXJ1 prevents cilia growth inhibition by cigarette smoke in human airway epithelium in vitro. Am J Respir Cell Mol Biol. 2014;51:688–700.
24. Wallmeier J, Frank D, Shoemark A, Nöthe-Menchen T, Cindric S, Olbrich H, et al. De novo mutations in FOXJ1 result in a motile ciliopathy with hydrocephalus and randomization of left/right body asymmetry. Am J Hum Genet. 2019;105:1030–9.
25. Yin W, Liontos A, Koepke J, Ghoul M, Mazzocchi L, Liu X, et al. An essential function for autocrine hedgehog signaling in epithelial proliferation and differentiation in the trachea. Development. 2022;149:dev199804.
26. Bodas M, Subramaniyan B, Moore AR, Metcalf JP, Ocañas SR, Freeman WM, et al. The NOTCH3 downstream target HEYL is required for efficient human airway basal cell differentiation. Cells. 2021;10:3215.
27. Bodas M, Moore AR, Subramaniyan B, Georgescu C, Wren JD, Freeman WM, et al. Cigarette smoke activates NOTCH3 to promote goblet cell differentiation in human airway epithelial cells. Am J Respir Cell Mol Biol. 2021;64:426–40.
28. Zahid M, Feinstein TN, Oro A, Schwartz M, Lee AD, Lo CW. Rapid Ex-Vivo ciliogenesis and dose-dependent effect of notch inhibition on ciliogenesis of respiratory epithelia. Biomolecules. 2020;10:1182.
29. Bergeron C, Tulic MK, Hamid Q. Tools used to measure airway remodelling in research. Eur Respir J. 2007;29:596–604.
30. Hogg JC, Chu F, Utokaparch S, Woods R, Elliott WM, Buzatu L, et al. The nature of small-airway obstruction in chronic obstructive pulmonary disease. N Engl J Med. 2004;350:2645–53.
31. Leopold PL, O'Mahony MJ, Lian XJ, Tilley AE, Harvey BG, Crystal RG. Smoking is associated with shortened airway cilia. PLoS ONE. 2009;4:e8157.
32. Chaumont M, Bernard A, Pochet S, Mélot C, El Khattabi C, Reye F, et al. High- wattage E-cigarettes induce tissue hypoxia and lower airway injury: a randomized clinical trial. Am J Respir Crit Care Med. 2018;198:123–6.
33. Singh KP, Lawyer G, Muthumalage T, Maremanda KP, Khan NA, McDonough SR, et al. Systemic biomarkers in electronic cigarette users: implications for noninvasive assessment of vaping-associated pulmonary injuries. ERJ Open Res. 2019;5:00182–2019.
34. Podguski S, Kaur G, Muthumalage T, McGraw MD, Rahman I. Noninvasive systemic biomarkers of e-cigarette or vaping use-associated lung injury: a pilot study. ERJ Open Res. 2022;8:00639–2021.
35. Belgacemi R, Luczka E, Ancel J, Diabasana Z, Perotin JM, Germain A, et al. Airway epithelial cell differentiation relies on deficient Hedgehog signalling in COPD. EBioMedicine. 2020;51:102572.
36. Schmid A, Sailland J, Novak L, Baumlin N, Fregien N, Salathe M. Modulation of Wnt signaling is essential for the differentiation of ciliated epithelial cells in human airways. FEBS Lett. 2017;591:3493–506.
37. Carlier FM, Dupasquier S, Ambroise J, Detry B, Lecocq M, Biétry-Claudet C, et al. Canonical WNT pathway is activated in the airway epithelium in chronic obstructive pulmonary disease. EBioMedicine. 2020;61:103034.
38. Komura M, Sato T, Yoshikawa H, Nitta NA, Suzuki Y, Koike K, et al. Propylene glycol, a component of electronic cigarette liquid, damages epithelial cells in human small airways. Respir Res. 2022;23:216.
39. Bergen V, Lange M, Peidli S, Wolf FA, Theis FJ. Generalizing RNA velocity to transient cell states through dynamical modeling. Nat Biotechnol. 2020;38:1408–14.
40. Leung C, Wadsworth SJ, Yang SJ, Dorscheid DR. Structural and functional variations in human bronchial epithelial cells cultured in air-liquid interface using different growth media. Am J Physiol Lung Cell Mol Physiol. 2020;318(5):L1063–73.

Publisher's Note